This is an unofficial copy of a technical report jointly published by Ford Motor Co. Scientific Research Laboratories, Dearborn Michigan and the Department of Mechanical Engineering at the University of Michigan, Ann Arbor, August 15 1991

OPTIMAL ENGINE DESIGN USING NONLINEAR PROGRAMMING AND THE ENGINE SYSTEM ASSESSMENT MODEL

by

Terrance C. Wagner (1)

and

Panos Y. Papalambros (2)

A Sequential Quadratic Programming optimization algorithm was interfaced to the Engine System Assessment (ESA) model to determine the optimal combustion chamber geometry to maximize power. Both net power and power per unit displacement were studied, together with packaging, fuel economy and knock limiting constraints. Sensitivity of the optimal solution to changes in constraint parameters was also studied. Changes in the fuel economy and the displacement volume specifications affected the optimal design. It is shown that the problem of optimizing power is one of maximizing bore without exceeding the package constraint and/or degrading fuel economy. Also, to optimize net power subject to package constraints, the displacement volume should be treated as a variable subject to package constraints and not specified a priori.

Two algebraic models are developed first,based on ESA expressions; one for a flat head design and one for a compound valve head design. They are used with monotonicity analysis to determine a partial solution analytically. The analytical results and the numerical results with the ESA program gave identical solutions for the geometric design variables. Absolute values of brake power and specific fuel consumption differed because the algebraic expressions contained incomplete friction models.

While the optimal designs concluded from this work may be readily apparent to experienced engine engineers, the readily available sensitivity of the optimal design to changes in constraint parameters is not. Therein lies the utility of the described approach. The optimization algorithm, the interface, and relevant future work are also described.

APPROVED: ____

R.J. Tabaczynski, Manager

Engine Research Department ______________________

(1) Engine Research Department, Research Staff

(2) Professor, Department of Mechanical Engineering and Applied Mechanics,

The University of Michigan, Ann Arbor, MI.

1. Introduction

Engine modeling activities at Ford have the long term goal of reducing product development time and cost and improving product value. By providing sufficiently accurate simulations these models enable engineers to assess the effects of engine design variables on both engine commodity objectives and, with the complementary use of the Corporate Vehicle Simulation Program (CVSP), the effects on vehicle objectives. Sufficiently accurate models can be used to seek optimal designs, but to date, the methods represent an arduous task for the user. An array of design variables is usually determined by the user and a batch file is built to run the given model with this array of inputs. The output is then regressed in terms of those variables and the optimum sought by the user. (See for example, the use of Taguchi Design of Experiments techniques by Kenney et.al. [1989].) This paper demonstrates the utility of incorporating numerical optimization methods into this process.

Specific advantages result from such an approach. The reduction of workload in seeking the optimum is the most obvious. With the appropriate interface of a model to an optimization software package the user can readily study design *solutions* by changing the set of design variables, the design objective and constraints, and examining the effects of widening or narrowing the constraint boundaries.

In this report, optimization techniques are used in internal combustion engine design to obtain preliminary values for a set of combustion chamber design variables that maximize power output per unit displacement volume while meeting specific fuel economy and packaging constraints. Two types of mathematical optimization models are used: an explicit algebraic model obtained by simplifying expressions found in the Engine System Assessment program [Belaire and Tabaczynski, 1985] and an optimization model which uses the Engine System Assessment program directly as a function generator. Two combustion chamber geometries are studied with the algebraic model, a simple flat head design and a compound valve head design.

The report is organized as follows. A brief review of the use of numerical optimization techniques (including applications to engine design) is provided. Next, the development of the explicit algebraic models are presented followed by some analysis on boundedness and constraint activity. Relevant features of the ESA model are described next. Computational results are then presented for both the algebraic models and the ESA program. Lastly, extensive parametric studies are presented to show how changes in parameter values affect the optimal design.

The work described here is preliminary. The advantages of extending these techniques to more detailed models like the Engine Simulator (ENGSIM) and the Corporate Vehicle Simulation Program (CVSP) should become apparent. ESA was selected as the first model because of its ease of use, its explicit algebraic expressions and its continued proliferation into the company operations.

2. Optimization Methods

The terms *objective, constraint, variable, parameter, vector,* and *feasible domain* have explicit definitions given below.

The *objective* is the quantity to be optimized (minimized or maximized). It can be an explicit algebraic function or it can be an output of another computer program .

A (design)*variable* is any quantity allowed to vary during the search for the optimum objective. At least the objective function or one of the constraints should depend on a variable; otherwise it is not relevant to the problem statement.

A *parameter* is any quantity appearing in the problem statement which is fixed during the optimization. For example, the values of the bounds appearing in the constraint set are parameters.

A *constraint* bounds the set of variables in some way. Examples are: upper and lower bounds on variables, equality relationships among variables, upper and lower bounds on explicit algebraic expressions relating design variables or upper and lower bounds on outputs of a model. The set of variable values bounded by the set of constraints is called the *feasible domain.*

A *vector* is simply a set of scalars. The set of variables is a vector; the set of equality constraints is a vector; the set of inequality constraints is a vector. Also recall from multivariable calculus that the gradient of a scalar is a vector; and that the gradient of a vector is a matrix.

2.1 Unconstrained Optimization

The goal of optimization is to minimize or maximize a single function *f*, which depends on one or more independent variables. The value of those variables at that minimum or maximum and the value of *f* is termed the *optimal solution*. The calculation of gradients in the design variable space in search of a minimum is the essence of the algorithms of interest here. For a comprehensive, understandable introduction to optimization see Chapter 10 of *Numerical Recipes - The Art of Scientific Computing,* [Press, et.al.,1987].

The classical statement of an unconstrained optimization problem is to minimize (or maximize) a function f which depends upon a vector, **x,** of n variables where $\mathbf{x} = \{x_1, x_2, \ldots\ldots, x_n,\}$. The statement of the problem for **x** is:

$$\text{minimize } f(\mathbf{x})$$
$$\mathbf{x} = \{x_1, x_2, \ldots\ldots, x_n,\} \ \varepsilon\ \mathrm{R}^n \qquad (1)$$

For a single variable problem, ($\mathbf{x} = \{x\}$) recall from calculus that the first order necessary condition for a minimum is $df/dx = 0$. Also recall that the value of d^2f/dx^2 at this value of x sufficiently determines whether the function is a minimum or maximum; it is called the second order sufficiency condition . Similarly, for a function of n variables the first order necessary condition is that the *gradient* of $f(\mathbf{x})$ be equal to zero. That is:

$$\nabla f(\mathbf{x}) = \begin{array}{ccc} \frac{\partial f}{\partial x_1} & = & 0 \\ \frac{\partial f}{\partial x_2} & = & 0 \\ \cdot & & \cdot \\ \cdot & & \cdot \\ \frac{\partial f}{\partial x_n} & = & 0 \end{array} \qquad (2)$$

This results in a set of n equations that must be solved. Newton's method is a straightforward algorithm to solve such a set of equations. The following steps describe the algorithm .

Step 1. Pick a starting point (a guess of the solution) $\mathbf{x}^0$ and set an iteration counter k = 0. (Superscript indicates iteration number).

Step 2. Calculate a step size, $\mathbf{d}^k$, to move in $\mathbf{x}$ where

$$\mathbf{d}^k = -[\mathbf{D}(\nabla f(\mathbf{x}))^k]^{-1} (\nabla f(\mathbf{x}))^k \qquad (3)$$

and $\mathbf{D}(\nabla f(\mathbf{x}))$ is the Jacobian of the gradient of $f(\mathbf{x})$ and the Hessian of $f(\mathbf{x})$.

Step 3. Calculate a new value of $\mathbf{x}$ using

$$\mathbf{x}^{k+1} = \mathbf{x}^k + \mathbf{d}^k \qquad (4)$$

Step 4. If a convergence criteria is satisfied (e.g. $\| \mathbf{x}^{k+1} - \mathbf{x}^k \| \leq \varepsilon$) stop; otherwise increment k by one and go to 2.

For quadratic functions, it can be shown that this method converges in one step from the starting point [Dennis et al., 1989].

2.2 Constrained Optimization

Most design problems have many constraints imposed. For example, engine design problems include geometric constraints on the engine package, and performance criteria constraints on the vehicle. The constraints can be in the form of an equality (e.g., π (bore)^2 x (stroke) - 4 (volume) = 0) or an inequality (e.g., (maximum piston speed) - 25m/sec $\leq$ 0). Each equality constraint equation is valued at 0 and is usually denoted by h. Similarly, inequalities are expressions set less than or equal to 0 and are denoted by g. Table I shows a formal statement of a constrained minimization problem .

Table 1. Example of Constrained Minimization Problem

minimize f (**x**)	$(x_1 + 3x_2 + x_3)^2 + 4(x_1 - x_2)^2$
subject to:	
$h_1(\mathbf{x}) = 0$	$1 - x_1 - x_2 - x_3 = 0$
$g_1(\mathbf{x}) \le 0$	$3 + x_1^3 - 4x_3 - 6x_2 \le 0$
$g_2(\mathbf{x}) \le 0$	$-x_1 \le 0$
$g_3(\mathbf{x}) \le 0$	$-x_2 \le 0$
$g_4(\mathbf{x}) \le 0$	$-x_3 \le 0$

In shorthand the formal statement of this problem is:

$$\begin{array}{ll} \text{min} & f(\mathbf{x}) \\ \text{subj. to :} & \mathbf{h}(\mathbf{x}) = \mathbf{0} \\ & \mathbf{g}(\mathbf{x}) \le \mathbf{0} \end{array} \qquad (5)$$

where $\mathbf{h}(\mathbf{x}) = \{h_1(\mathbf{x}), h_2(\mathbf{x}), ..., h_m(\mathbf{x})\}$ is a vector of equality constraints and $\mathbf{g}(\mathbf{x}) = \{g_1(\mathbf{x}), g_2(\mathbf{x}), ..., g_l(\mathbf{x})\}$ is a vector of inequality constraints.

2.2.1 The Lagrangian

A class of algorithms have been developed to solve this problem by minimizing a scalar function called the Lagrangian. It is a weighted sum of the objective function and the constraints. The weights are multipliers for each of the constraints. There are l multipliers for the equality constraints, $\lambda = (\lambda_1, \lambda_2, ... \lambda_l)$ and m multipliers for the inequality constraints, $\mu = (\mu_1, \mu_2, ... \mu_m)$. Hence λ and μ are vectors. The Lagrangian is written as

$$L = f(\mathbf{x}) + \sum_l \lambda_i \, h_i(\mathbf{x}) + \sum_m \mu_i \, g_i(\mathbf{x}) \qquad (6)$$

and the optimization problem is stated as

$$\begin{array}{ll} \text{minimize} & L(\mathbf{x}) \\ \text{subject to:} & \mu \ge \mathbf{0} \\ & \lambda \ne \mathbf{0}. \end{array} \qquad (7)$$

Formulation of the Lagrangian transforms a constrained minimization problem into an equivalent unconstrained minimization problem.

2.2.2 The Karush-Kuhn-Tucker (KKT) Conditions

The first order necessary condition for the minimization of the Lagrangian is that the gradient of the Lagrangian be equal to zero. (For proof see for example, Dennis et al. [1989]).

$$\nabla L = \nabla f(\mathbf{x}) + \mu^T \nabla \mathbf{h}(\mathbf{x}) + \lambda^T \nabla \mathbf{g}(\mathbf{x}) = \mathbf{0}^\mathbf{T} \qquad (8)$$

In addition, the following must hold.

$$\begin{aligned} &\lambda \neq \mathbf{0} \\ &\mu \geq \mathbf{0} \\ &\lambda^\mathbf{T}\, \mathbf{h}(\mathbf{x}) = \mathbf{0}^\mathbf{T} \\ &\mu^\mathbf{T}\, \mathbf{g}(\mathbf{x}) = \mathbf{0}^\mathbf{T} \end{aligned} \qquad (9)$$

These are called the Karush-Kuhn-Tucker (KKT) conditions. and constitute the first order necessary conditions for the constrained optimization problem. One class of algorithms to solve this problem is called Sequential Quadratic Programming (SQP) and is described briefly below. See Papalambros and Wilde [1988] or Luenberger [1984] for a more detailed discussion of SQP methods.

2.3 Sequential Quadratic Programming (SQP) Methods

SQP methods approximate the gradient of the Lagrangian with a first order Taylor's expansion. This is equivalent to approximating the Lagrangian as a quadratic function. The constraints are approximated with a linear approximation. An iterative algorithm to solve

$$\nabla L(\mathbf{x}) = \mathbf{0}$$

results in solving a sequence of quadratic programming subproblems; hence the name SQP. The solution of the quadratic subproblem yields a step *direction* for the next iteration in the design space. In addition, a line search algorithm is usually invoked to determine the best magnitude for the direction found.

2.4 Optimal Engine Design Studies

Optimization algorithms have been in use for some time to determine optimal control schedules of air-fuel ratio, spark and exhaust gas recirculation as a function of speed and torque to meet fuel and emissions requirements of the Environmental Protection Agency (EPA) driving cycle (see for example, Auiler et al. [1978]; Rishavy et al. [1977]). Physically based models of the combustion process in internal combustion engines have been in use for over a decade (Blumberg et al. [1980], Heywood [1980]; Kreiger [1980]; Reynolds [1980]) to predict the effects of relevant design changes in combustion chamber, valve/port interface, and valve timing (Davis and Borgnakke [1981], Davis et al. [1986, 1988]; Newman et al. [1989]). However, optimal designs are still sought primarily through arduous studies varying one variable at time. These studies usually involve a series of hill-climbing (or descending) algorithms which are both computationally expensive and non-convergent from the optimization viewpoint [Kenney et al. 1989, Luenberger 1984].

Kenney et al. [1989] discuss the use of design of experiments techniques to specify the operating conditions for a parametric study, and use the General Engine Simulator to optimize cam event timing for improving idle stability of a 5.8L gasoline engine. They used the same technique to optimize cam timing for wide open throttle performance using Ford’s one-dimensional compressible flow model of the manifold fluid dynamics (MANDY, see Chapman et al. [1982] for model description). Upper and lower variable bounds were the only constraints in both problems. Assanis and Polishak [1989] used the model of Poulos and Heywood [1983] to predict optimal cam timing. They predicted and experimentally verified a 5% increase in peak torque. Woodard et al. [1988] formulated and solved a nonlinear programming problem using Campbell's model [1979] with a general conjugate gradient method to minimize fuel consumption at a single operating condition representing vehicle cruise. They varied combustion chamber geometry and valve timing and predicted a 20% reduction in fuel consumption over the existing design. A clever technique for accommodation of the discrete cam timing variables was also presented.

The work described above was directed at improving existing designs using detailed models that numerically integrate the energy equation for a full thermodynamic Otto cycle. The work here presents the preliminary engine design problem as a nonlinear programming problem using a "lumped" thermodynamic model as expressed in the technical appendix for the Engine System Assessment program [Belaire and Tabaczynski, 1985] ; similar empiricisms can be found in the open literature (see for example, Bishop [1964]; Taylor [1985]; Heywood [1988]).

The utility of such a model is to obtain an expedient first order approximation to the optimal engine configuration and the sensitivity of the optimum to changes in problem parameters, such as package size and structural or manufacturability design rules. Such analysis is essential to efficiently allocate resources for optimal camshaft, port, piston, and valvetrain design with models of appropriate detail. In addition, an identical strategy, with appropriate resources, can be applied to the execution of more complex programs such as ENGSIM and CVSP.

3. The Optimization Problem Statement

The engine design problem is stated as a non-linear programming (NLP) problem in the so-called negative null form of Equation (5). Explicit relationships are derived for the objective function, equality constraints, and inequality constraints. As outlined above, f, h, and g can be explicitly represented as functions of the design variables or implicitly as output from another program. Section 3.1 outlines the development of the explicit mathematical optimization models for two combustion chamber head geometries, flat and compound valve. Both models are extracted from the algebraic expressions in the ESA Technical Appendix; readers familiar with ESA can skip section 3.1 without loss of continuity. Section 3.2 presents a monotonicity analysis [Papalambros and Wilde, 1988] of the algebraic expressions. Sections 3.3 - 3.5 show how the NLP problem is formulated calling ESA as a subroutine.

3.1 Development of the Algebraic Models

These explicit models begin with an expression for the ideal thermal efficiency using the basic air-cycle definition, and then adjust that to account for air-fuel effects, including exhaust gas recirculation and combustion time losses. The resulting thermal efficiency value is further corrected for heat transfer losses in the engine and for engine speed effects.

The optimization objective is to maximize brake power or brake power per unit engine displacement, while meeting packaging and fuel economy constraints. The symbols used in the models are summarized in the nomenclature, Table 2.

3.1.1 Model A - Flat Head Combustion Chamber

The assumed geometry for the flat head design is shown in Figure 1. The objective is to maximize the brake power per unit engine displacement, BKW/V, given by

$$BKW/V = K_0(BMEP)w \qquad (10)$$

where $K_0 = 1/120$ is a unit conversion constant and

$$BMEP = IMEP - FMEP \qquad (11)$$

Here BMEP, IMEP, and FMEP are brake, indicated and friction mean effective pressures, respectively, and w is revolutions per minute divided by 1000.

The IMEP is computed from

$$IMEP = \eta_t \eta_v (\rho Q/A_f) \qquad (12)$$

where η_t is the thermal efficiency, η_v is the volumetric efficiency, ρ is the density of inlet charge, Q is the lower heating value of fuel, and A_f is the air-fuel ratio. The term $(\rho Q/A_f)$ is the amount of energy available in the air-fuel mixture per unit volume. The volumetric efficiency accounts for flow losses and the product $\eta_v(\rho Q/A_f)$ is the energy per unit volume available in the mass inducted into the combustion chamber. The thermal efficiency accounts for the thermodynamics associated with the Otto cycle.

Table 2. Nomenclature for Engine Model

A_f	air/fuel ratio
b	cylinder bore, mm
BKW	brake power, kW
BMEP	brake mean effective pressure, kPa
c_r	compression ratio
C_s	port discharge coefficient
d_E	exhaust valve diameter, mm
d_I	intake valve diameter, mm
EGR	exhaust gas recirculation, percent
FMEP	friction mean effective pressure, bars
h	compound valve chamber deck height, mm
H	distance dome penetrates head, mm
IMEP	indicated mean effective pressure, kPa
isfc	indicated specific fuel consumption, g/kwh
MAP	manifold absolute pressure, kPa
N_c	number of cylinders
N_v	number of valves
Q	lower heating value of fuel, kJ/kg
r	radius of compound valve chamber curvature, mm
s	stroke of piston, mm
S_v	surface to volume ratio, mm^{-1}
V, v	displacement volume, mm^3
v_c	clearance volume, mm^3
v_d	dome volume, mm^3
V_p	mean piston speed, m/min
w	revolutions per minute at peak power , x 10^{-3}
Z_b	RPM factor in volumetric efficiency
Z_n	Mach Index of port/chamber design
γ	ratio of specific heats of in-cylinder gases
η_v	volumetric efficiency
η_{vb}	base volumetric efficiency
η_t	thermal efficiency
η_{tad}	adiabatic thermal efficiency
η_{tw}	thermal efficiency at representative part load point (1500 rpm, A_f = 14.6)
ρ	density of inlet charge, kg/m^3
ϕ	equivalence ratio

The volumetric efficiency can be expressed as

$$\eta_v = \eta_{vb} (1 + Z_b^2)/(1 + Z_n^2) \qquad (13)$$

where η_{vb} is the base volumetric efficiency, Z_b is the RPM factor in volumetric efficiency, and Z_n is the Mach Index of port/chamber design. The base volumetric efficiency for a "best-in-class" engine may be expressed empirically with a curve-fitting formula in terms of RPM at peak power, w, as follows:

$$\eta_{vb} = 1.067 - 0.038\, e^{w-5.25} \qquad \text{for } w \geq 5.25$$

$$\eta_{vb} = 0.637 + 0.13w - 0.014w^2 + 0.00066w^3 \qquad \text{for } w \leq 5.25 \qquad (14)$$

Also empirically [Taylor 1985], for a speed of sound of 353 m/sec we set

$$Z_b = 7.72\,(10^{-2})w \qquad (15)$$

$$Z_n = 9.428\,(10^{-5})\, ws(b/d_I)^2 / C_s \qquad (16)$$

where s is the piston stroke, b is the cylinder bore, d_I is the intake valve diameter and C_s is the port discharge coefficient, a parameter characterizing the flow losses of a particular manifold and port design.

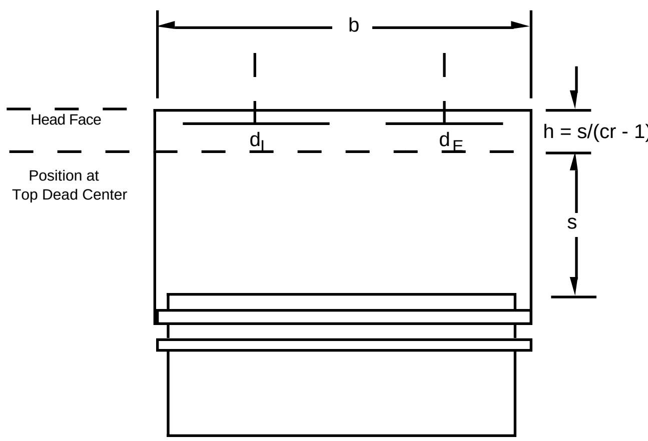

Figure 1. Schematic of geometry for flat head design

The thermal efficiency is expressed as

$$\eta_t = \eta_{tad} - .083\, S_v(1.500/w)^{0.5} \qquad (17)$$

where η_{tad} is the adiabatic thermal efficiency given by

$$\eta_{tad} = 0.9\,(1-c_r^{(1-\gamma)})(1.18 - 0.225\phi) \qquad \text{for } \phi \leq 1$$

$$= 0.9\,(1-c_r^{(1-\gamma)})(1.655 - 0.7\phi) \qquad \text{for } \phi > 1 \qquad (18)$$

and the S_v term accounts for heat transfer effects due to surface/volume ration of the chamber. Here c_r is the compression ratio, γ is the ratio of specific heats of the in-cylinder gases, and ϕ is the equivalence ratio that accommodates air-fuel ratios different from stoichiometric. In the optimal design model stoichiometry will be assumed, so that $\phi = 1$ and the two expressions in Eq.(18) will give the same result. The thermal efficiency for an ideal Otto cycle would be $(1-c_r^{(1-\gamma)})$. The 0.9 multiplier in the formulas accounts empirically for the fact that the heat release occurs over finite time, rather than instantaneously as in an ideal cycle, and it is assumed valid for displacements on the order of 400 to 600 cc/cylinder and bore-to-stroke ratios between 0.7 and 1.3 [Belaire and Tabaczynski, 1985]. Heat transfer is accounted for by the product of the surface-to-volume ratio of the cylinder, S_V, and an RPM correction factor. The surface-to-volume ratio is expressed as

$$S_V = [(0.83)\,(12s + (c_r - 1)(6b + 4s))]/[bs\,(3 + (c_r - 1))] \qquad (19)$$

for a reference speed of 1500 rpm and 4.14 bar of IMEP.

Finally the FMEP is derived with the simple assumption that the operating point of interest will be near wide open throttle, the point used for engine power tests, and that engine accessories are ignored. Under these conditions pumping losses are small and ignored. The primary factors affecting engine friction are compression ratio and engine speed. An expression to reflect this is

$$\text{FMEP} = (4.826)(c_r - 9.2) + (7.97 + 0.253V_p + 9.7(10^{-6})V_p^2) \qquad (20)$$

where V_p is the mean piston speed. More complete expressions (e.g., Bishop 1964, Patton et al. 1989) were not employed in order to keep the monotonicity analysis of the algabraic model tractable.

The constraints included are packaging and efficiency constraints. The packaging constraints are as follows. We chose the maximum length of the engine block to be L_1 = 400 mm. This limit constrains the bore using the practical design rule that the distance separating the cylinders should be greater than a certain percentage of the bore dimension. Therefore, for an in-line engine

$$K_1 N_c b \le L_1 \qquad (21)$$

where the constant K_1 = 1.2 for a cylinder separation of at least 20% of the bore, and N_c is the number of cylinders in the block. Similarly, engine height limit of L_2 = 200 mm constrains the stroke:

$$K_2 s \le L_2 \qquad (22)$$

where K_2 = 2. For a flat cylinder head, geometric and structural constraints require the intake and exhaust valve diameters to satisfy the relationship

$$d_I + d_E \le K_3 b \qquad (23)$$

where K_3 = 0.82, and the ratio of exhaust valve to inlet valve diameter is restricted as

$$K_4 \le d_E/d_I \le K_5 \qquad (24)$$

where K_4 = 0.83 and K_5 = 0.87. Finally, the displacement volume is a given parameter related to design variables by

$$V = \pi N_c b^2 s/4 \tag{25}$$

We now examine efficiency-related constraints. To preclude significant flow losses due to compressibility of the air-fuel charge during induction the Mach Index of port/chamber design must be less than K_6 = 0.6 [Taylor 1985]:

$$Z_n = 9.428\,(10^{-5})\, ws(b/d_I)^2 /C_s \le K_6 \tag{26}$$

Knock-limited compression ratio for 98 octane fuel can be represented by [Heywood 1988]:

$$c_r \le 13.2 - 0.045b \tag{27}$$

The rated RPM at which maximum power occurs should not exceed the limits of the torque converter in conventional automatic transmissions, K_7 = 6.5 (x1000 rpm). Therefore,

$$w \le K_7. \tag{28}$$

Fuel economy at part load (1500 rpm , A_f = 14.6) is a representative restriction on overall fuel economy. Therefore, a constraint is imposed on the indicated specific fuel consumption, isfc, at this part load:

$$isfc = 3.6\,(10^6)\,(\eta_{tw}\, Q)^{-1} \le K_8 \tag{29}$$

where η_{tw} is the part-load thermal efficiency and K_8 = 230.5 g/kWh.

In order to assign parameter values, we select specifications for a 1.86L four- cylinder engine. For this engine configuration maximizing power density is important. The following values are then used for the parameters.

$$\begin{array}{lll} \rho = 1.225\ \text{kg/m}^3 & \gamma = 1.33 & V = 1.859\,(10^6)\ \text{mm}^3 \\ Q = 43958\ \text{kJ/kg} & N_c = 4 & C_s = 0.44 \\ A_f = 14.6 & & \end{array} \tag{30}$$

The ratio of specific heats is computed from the expression

$$\gamma = 1.33 + 0.01\,(EGR/30) \tag{31}$$

with zero recirculation assumed, so γ = 1.33.

The expression for thermal efficiency (and hence also fuel consumption) uses a single multiplier to account for time losses related to flame propagation rates. The value of 0.9 in Eq.(18) is considered valid within the limited range of bore-to-stroke ratios of

$$0.7 \le b/s \le 1.3 \tag{33}$$

Outside this range, the geometry significantly affects flame propagation. Presumably, a dependence of the multiplier on bore-to-stroke ratio could be developed and used. This was not done in the present model, so Eq. (33) is treated as a set constraint, not included explicitly in the model but checked after results have been obtained. Also note that the treatment of C_s as a parameter implies C_S is independent of valve size. This assumption requires scrutiny if Equation (23) is not satisfied as a strict equality.

The model is now assembled after elimination of the stroke variable using the equality constraint on displacement volume, Equation (25), and is cast into a standard NLP form, the objective being to minimize *negative* specific power (BKW/V).

MODEL A (34)

Minimize $f = K_0(\text{FMEP} - (\rho Q/A_f)\,\eta_t\eta_v)\,w$ (in kW/liter)

where

$\eta_v = \eta_{vb}\,[1 + 5.96\text{x}10^{-3}\,w^2]/[1 + [(9.428\text{x}10^{-5}(4V/\pi N_c C_s)(w/d_I^{\,2})]^2]$

$\eta_{vb} = 1.067 - 0.038e^{w-5.25}$ for $w \geq 5.25$

$= 0.637 + 0.13\,w - 0.014\,w^2 + 0.00066w^3$ for $w \leq 5.25$

$\eta_t = \eta_{tad} - S_v(1.5/w)^{0.5}$

$\eta_{tad} = 0.8595\,(1 - c_r^{-0.33})$

$S_v = (0.83)\,[(8 + 4c_r) + 1.5(c_r - 1)(\pi N_c/V)b^3]/[(2 + c_r)b]$

$\text{FMEP} = (4.826)(c_r - 9.2) + (7.97 + 0.253\,V_p + 9.7(10^{-6})V_p^{\,2})$

$V_p = (8V/\pi N_c)wb^{-2}$

subject to

$g_1 = K_1 N_c b - L_1 \leq 0$	min bore wall thickness
$g_2 = (4K_2 V/\pi N_c L_2)^{1/2} - b \leq 0$	max engine height
$g_3 = d_I + d_E - K_3 b \leq 0$	valve geometry and structure
$g_4 = K_4\,d_I - d_E \leq 0$	min valve diameter ratio
$g_5 = d_E - K_5\,d_I \leq 0$	max valve diameter ratio
$g_6 = (9.428)(10^{-5})(4V/\pi N_c)(w/d_I^{\,2}) - K_6 C_s \leq 0$	max port/chamber Mach Index
$g_7 = c_r - 13.2 + 0.045\,b \leq 0$	knock-limited compression ratio
$g_8 = w - K_7 \leq 0$	max torque converter rpm
$g_9 = 3.6\,(10^6) - K_8 Q\eta_{tw} \leq 0$	min fuel economy at part load

where $\eta_{tw} = 0.8595\,(1 - c_r^{-0.33}) - S_v$

This concludes the initial modeling effort for the flat head design problem. Note that there are five design variables, b, d_I, d_E, c_r, and w. There are nine inequality and no equality constraints, as all equalities that appear in Model A are simple definitions of intermediate quantities appearing in the inequalities. Significant parameters, for which numerical values were given in Equation (30), are maintained in Model A with their symbols for easy reference in subsequent parametric post-optimality studies. Parameter values dictated by current practice or given design specifications are indicated by the K_i (i = 1,..., 12) and L_i (i = 1, 2) coefficients and summarized in Table 3.

3.1.2 Model B - Compound Valve Head Chamber Geometry

The geometry for the compound valve head design is shown in Figure 2. Accounting for this new geometry will change Model A presented above with the addition of new design variables and constraints. The new variables are the displacement volume v (considered a parameter in Model A), the deck height h, and the radius of curvature r. As displacement is now a variable, the objective function is selected to be brake power rather than specific brake power. A relationship between clearance volume v_c, displacement volume v, and compression ratio is imposed by the definition of the compression ratio:

$$c_r = (v/N_c + v_c)/v_c \qquad (35)$$

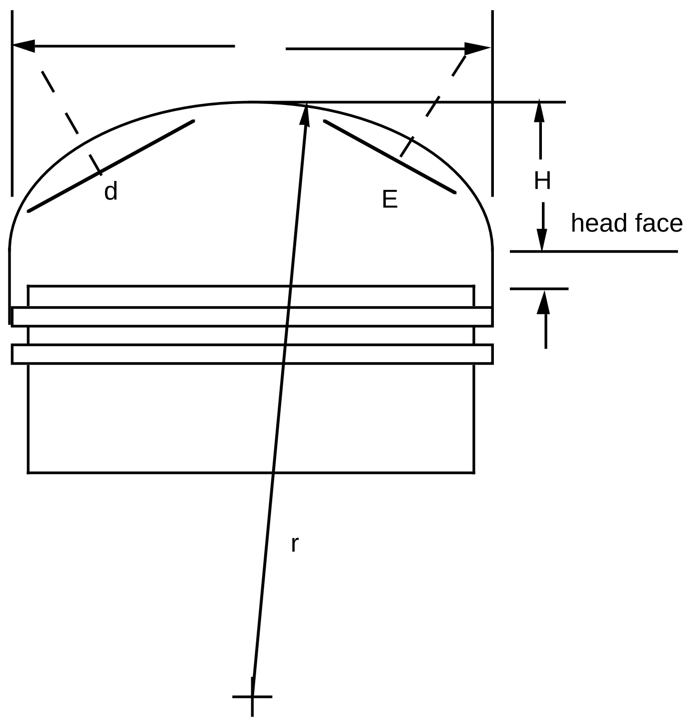

Figure 2. Schematic for compound valve design

The clearance volume is the sum of deck volume and dome volume v_d.

$$v_c = \pi h b^2/4 + v_d \qquad (36)$$

where

$$v_d = (1/3)\pi[(r^2 - b^2/4)^{1.5} - (r^2 - d_I{}^2/4)^{1.5} - (r^2 - d_E{}^2/4)^{1.5}]$$
$$- \pi r^2[(r^2 - b^2/4)^{0.5} - (r^2 - d_I{}^2/4)^{0.5} - (r^2 - d_E{}^2/4)^{0.5}] - (2/3)\pi r^3 \qquad (37)$$

A typical design specification on the deck height is

$$h = K_{11}b \quad (38)$$

where K_{11} = 1/64. A minimum distance of $K_{12}b$ must separate the two valves (Taylor 1985), where K_{12} = 0.125. Geometrically this can be approximated by setting

$$(d_I^2 - H^2)^{0.5} + (d_E^2 - H^2)^{0.5} \leq (1 - K_{12})\, b \quad (39)$$

where H is the distance the dome penetrates the head (Figure 2) and is defined as

$$H = r - (r^2 - b^2/4)^{0.5} \quad (40)$$

In standard NLP form the problem of maximizing power for the compound valve head geometry becomes

MODEL B (41)

Minimize $f = K_0(FMEP - (\rho Q/A_f)\, \eta_t \eta_v)\, wv$

where

$\eta_v = \eta_{vb}\,[1 + 5.96x10^{-3}\, w^2]/[1 + [(9.428x10^{-5}(4v/\pi N_c N_v C_s)(w/d_I^2)]^2]$

$\eta_{vb} = 1.067 - 0.038e^{w-5.25}$ for $w \geq 5.25$

$= 0.637 + 0.13\, w - 0.014\, w^2 + 0.00066 w^3$ for $w \leq 5.25$

$\eta_t = \eta_{tad} - S_v(1.5/w)^{0.5}$

$\eta_{tad} = 0.9\, (1 - c_r^{-0.33})(1.18 - 0.225\phi)$ for $\phi \leq 1$

$= 0.9\, (1 - c_r^{-0.33})(1.655 - 0.7\phi)$ for $\phi > 1$

$S_v = (0.83)\, [(8 + 4c_r) + 1.5(c_r - 1)(\pi N_c/v)b^3]/[(2 + c_r)b]$

$FMEP = (4.826)(c_r - 9.2) + (7.97 + 0.253\, V_p + 9.7(10^{-6})V_p^2)$

$V_p = (8v/\pi N_c)wb^{-2}$

subject to:

$h_1 = c_r - (v/N_c + v_c)/v_c = 0$ compression ratio definition

where $v_c = \pi hb^2/4 + v_d$

$v_d = (1/3)\pi[(r^2 - b^2/4)^{1.5} - (r^2 - d_I^2/4)^{1.5} - (r^2 - d_E^2/4)^{1.5}]$
$- \pi r^2[(r^2 - b^2/4)^{0.5} - (r^2 - d_I^2/4)^{0.5} - (r^2 - d_E^2/4)^{0.5}] - (2/3)\pi\, r^3$

$h_2 = h - K_{11}b = 0$ deck height specification

$g_1 = K_1 N_c b - L_1 \leq 0$ min bore wall thickness

$g_2 = (4K_2 v/\pi N_c L_2)^{1/2} - b \leq 0$ max engine height

$g_3 = (d_I^2 - H^2)^{0.5} + (d_E^2 - H^2)^{0.5} - K_{3c}b \leq 0$ min valve distance

where $H = r - (r^2 - b^2/4)^{0.5}$

$g_4 = K_4\, d_I - d_E \leq 0$ min valve diameter ratio

$g_5 = d_E - K_5\, d_I \leq 0$ max valve diameter ratio

$g_6 = (9.428)(10^{-5})(4v/\pi N_c)(w/d_I^2) - K_6 C_s \leq 0$ max port/chamber Mach Index

$g_7 = c_r - 13.2 + 0.045\, b \le 0$	knock-limited compression ratio
$g_8 = w - K_7 \le 0$	max torque converter rpm
$g_9 = 3.6\,(10^6) - K_8 Q \eta_{tw} \le 0$	min fuel economy at part load
where $\eta_{tw} = 0.8595\,(1 - c_r^{-0.33}) - S_v$	
$g_{10} = v - K_9 \le 0$	
$g_{11} = -v + K_{10} \le 0$	

The empirical parameters have the same values as in Model A in addition to $K_{3c} = 1 - K_{12} = 0.875$, $K_9 = 1.6(10^6)$, $K_{10} = 2.3(10^6)$. There are two equality constraints (h_1 and h_2) added to this model. In principle, one design variable can be eliminated for each equality (e.g. cr, and h). However, this creates an algebraic nightmare for the other contraints, so no model reduction will be attempted using the equality constraints. Constraint g_3 has been rewritten and two additional inequalities, g_{10} and g_{11}, have been added to provide upper and lower bounds on the displacement volume.

Table 3. Current Practice or Design Specification Parameters

PARAMETER	VALUE	SPECIFICATION
K_0	1/120	unit conversion, 4 stroke engine
K_1	1.2	cylinder separation as % of bore
K_2	2	engine height as a multiple of stroke
K_3	0.82	valve spacing as % of bore (flat head)
K_4	0.83	lower bound on valve ratio
K_5	0.89	upper bound on valve ratio
K_6	0.6	upper bound on Mach Index
K_7	6.5	upper bound on rpm
K_8	230.5 g/kWh	upper bound on isfc
K_9	$2.3\,(10^6)\text{mm}^3$	upper bound on displacement volume
K_{10}	$1.6\,(10^6)\text{mm}^3$	lower bound on displacement volume
K_{11}	1/64	bore fraction specification for deck height
K_{12}	0.125	bore fraction specification for valve distance
L_1	400 mm	upper bound on engine block length
L_2	200 mm	upper bound on engine block height

3.2 Monotonicity Analysis

In many design models, the objective and constraint functions are *monotonic* with respect to the design variables. A continous differentiable function f(**x**) is *monotonically increasing* with respect to (wrt) a design variable x_i, if $\partial f/\partial x_i > 0$; it is *monotonically decreasing* wrt a design variable x_i, if $\partial f/\partial x_i < 0$. Under either condition, we say that f is coordinate-wise monotonic wrt x_i, or that x_i is a monotonic variable in f. Monotonicity analysis is a model analysis methodology that checks whether a model is properly bounded and identifies active constraints when possible. Active inequality constraints must be satisfied as strict equalities at the optimum and they correspond to critical design requirements. See Papalambros and Wilde (1988) for further details.

We start monotonicity analysis of Model A by identifying any monotonicities in the model functions. Examining the model we observe the following.

$$FMEP = FMEP(c_r\,,\, V_p^{+}(w^{+}, b^{-})) = FMEP(c_r, w^{+}, b^{-})$$
$$\eta_t = \eta_t(c_r^{+}, S_V^{-}(c_r,\ b^{+})) = \eta_t(c_r, b^{-}) \qquad (42)$$
$$\eta_V = \eta_V(w, d_I^{+})$$

In Equation (42) the right hand side shows how the functions on the left depend on the design variables. A superscript sign indicates the type of monotonicity that may exist, positive (or negative) indicating that the function is increasing (or decreasing) wrt to that variable; no sign indicates that the variable has undetermined monotonicity. All monotonicities above are easy to verify except that wrt b. Although the proof is omitted here, it is worth noting that it is a *regional* monotonicity, namely, valid only for the range of design variable values within the feasible domain.

The monotonicities of Model A can be now presented as follows.

MODEL A1 (43)

$$\min f(c_r, w, b, d_I^{-}) = K_0 w\,[FMEP(c_r, w^{+}, b^{-}) - P_0\, \eta_t(c_r, b^{-})\, \eta_V(w, d_I^{+})]$$

subject to

$g_1(b^{+}) = b - P_1 \le 0$	min bore wall thickness
$g_2(b^{-}) = P_2 - b \le 0$	max engine height
$g_3(b^{-}, d_E^{+}, d_I^{+}) = d_I + d_E - K_3 b \le 0$	valve geometry and structure
$g_4(d_E^{-}, d_I^{+}) = K_4 d_I - d_E \le 0$	min valve diameter ratio
$g_5(d_E^{+}, d_I^{-}) = d_E - K_5 d_I \le 0$	max valve diameter ratio
$g_6(w^{+}, d_I^{-}) = P_3 w - d_I^2 \le 0$	max port/chamber Mach Index

$g_7(c_r^+, b^+) = c_r - 13.2 + 0.045\, b \leq 0$ knock-limited compression ratio

$g_8(w^+) = w - K_7 \leq 0$ max torque converter rpm

$g_9(c_r, b^+) = P_4 - 0.8595(1 - c_r^{-0.33}) + S_v(c_r, b^+) \leq 0$ min fuel economy at part load

Note that in this new model all known monotonicities are indicated and several *parametric relations* P_i have been introduced to simplify the presentation of the model. These are given in Table 4, the numerical values corresponding to parameter values for the base case. We now proceed with representing this information in a *monotonicity table*, as shown in Table 5.

Table 4. Parametric Functions for Model A

$P_0 = \rho Q/A_f = 3688$ kPa

$P_1 = L_1/K_1 N_c = 83.33$ mm

$P_2 = (4K_2V/\pi N_c L_2)^{1/2} = 76.90$ mm

$P_3 = 9.428\text{x}10^{-5}\,(4V/\pi N_c)/(K_6 C_s) = 215.5\ \text{mm}^2\text{sec}$

$P_4 = 3.6(10^6)/K_8 Q = .3412$

Table 5. Monotonicity Table for Model A1

	c_r	w	b	d_E	d_I
f	**U**	**U**	**U**		-
g_1			+		
g_2			-		
g_3			-	+	+
g_4				-	+
g_5				+	-
g_6		+			-
g_7	+		-		
g_8		+			
g_9	**U**		+		

In the monotonicity table the columns are the design variables and the rows are the objective and constraint functions, the entries in the table being the monotonicities of each function with respect to each variable. Positive (negative) sign indicates increasing (decreasing) function, U indicates undetermined or unknown monotonicity. An *empty* entry indicates that the function does not depend on the respective variable, so the table acts also as an incidence table.

The *Monotonicity Principles* can be more readily applied using the monotonicity table. These principles state the following (Papalambros and Wilde 1988):

First Monotonicity Principle (MP1): In a well-constrained objective function every increasing (decreasing) variable is bounded below (above) by at least one active constraint.

Second Monotonicity Principle(MP2): Every monotonic variable not occurring in a well-constrained objective function is either irrelevant and can be deleted from the problem together with all constraints in which it occurs, or is relevant and bounded by two active constraints, one from above and one from below.

Based on these principles and Table 5 the following conclusions are reached. By MP1 wrt d_I at least one of g_3 or g_4 must be active. We examine these two cases. (i) If g_3 is active, then by MP2 wrt d_E g_4 must be active as well. (ii) If g_4 is active, then by MP2 wrt d_E g_3 and/or g_5 must be active. But g_5 and g_4 cannot be simultaneously active because they represent upper and lower bounds on the same quantity. Therefore in case (ii) g_4 must be active also. We see that in either case, both g_3 and g_4 must be active at the optimum. This is a necessary optimality condition that must be satisfied by any subsequent numerical results. Solving for d_E and d_I in terms of the optimal value b^* (asterisk denotes optimal value) we get

$$d_E^* = b^* K_3 K_4/(1+K_4)$$
$$d_I^* = b^* K_3/(1+K_4) \qquad (44)$$

a solution that is acceptable provided $K_4 \leq K_5$. Note that g_5 is then inactive. Using the second of Equation (44) to eliminate d_I from the objective and remaining constraints Model A1 is now reduced to

MODEL A2 (45)

$$\min f(c_r, w, b) = K_0 w\ [FMEP(c_r, w^+, b^-) - P_0\ \eta_t(c_r, b^-)\ \eta_v(w, b^+)]$$

subject to

$g_1(b^+) = b - P_1 \leq 0$	min bore wall thickness
$g_2(b^-) = P_2 - b \leq 0$	max engine height
$g_6(w^+, b^-) = P_3 w - [K_3/(1+K_4)]^2 b^2 \leq 0$	max port/chamber Mach Index
$g_7(c_r^+, b^+) = c_r - 13.2 + 0.045\ b \leq 0$	knock-limited compression ratio

$g_8(w^+) = w - K_7 \le 0$ max torque converter rpm

$g_9(c_r, b^+) = P_4 - 0.8595(1- c_r^{- 0.33}) + S_v(c_r, b^+) \le 0$

min fuel economy at part load

where asterisks are dropped for convenience. There are only three design variables left and at most three constraints from the six in Model A2 can be active.

We proceed with monotonicity analysis for Model B. We now have

$$FMEP = FMEP(c_r , V_p^+(w^+, b^-, v^+)) = FMEP(c_r, w^+, b^-, v^+)$$

$$\eta_t = \eta_t(c_r^+, S_v^-(c_r, b^+, v^-)) = \eta_t(c_r, b^-, v^+) \quad (46)$$

$$\eta_v = \eta_v(w, d_I^+, v^-)$$

$$v_d = v_d(b, d_I^-, d_E^-, r)$$

The algebraic expression for v_d in Equation (37) is not easy to use for proving the monotonicities wrt d_I and d_E indicated above, but the geometry in Figure 2 shows that this is evidently the case. Eliminating variable h and constraint h_2 we get

MODEL B1 (47)

$$\min f(c_r, w, b, d_I^-, v) = K_0 wv\ [FMEP(c_r, w^+, b^-, v^+) - P_0\, \eta_t(c_r, b^-, v^+)\, \eta_v(w, d_I^+, v^-)]$$

subject to

$h_1(c_r^+, v^-, v_C^-) = - 1 + c_r - (v /N_C v_C) = 0$ head geometry

where $v_C = \pi K_{11} b^3/4 + v_d(b, d_I^-, d_E^-, r)$

$g_1(b^+) = b - P_1 \le 0$ min bore wall thickness

$g_2(b^-, v^+) = P_{2C}\, v^{1/2} - b \le 0$ max engine height

$g_3(b, d_E^+, d_I^+, r) \le 0$ valve geometry and structure

$g_4(d_E^-, d_I^+) = K_4 d_I - d_E \le 0$ min valve diameter ratio

$g_5(d_E^+, d_I^-) = d_E - K_5 d_I \le 0$ max valve diameter ratio

$g_6(w^+, d_I^-, v^+) = P_{3C} wv - d_I^2 \le 0$ max port/chamber Mach Index

$g_7(c_r^+, b^+) = c_r - 13.2 + 0.045\, b \le 0$ knock-limited compression ratio

$g_8(w^+) = w - K_7 \le 0$ max torque converter rpm

$g_9(c_r,b^+,v^+)=P_4 - 0.8595(1- c_r^{- 0.33})+S_v(c_r,b^+,v^+) \le 0$

min fuel economy at part load

$g_{10}(v^+) \leq 0$

$g_{11}(v^-) \leq 0$

where the revised parametric functions are

$$P_{2C} = (4K_2/\pi N_c L_2)^{1/2} \qquad P_{3C} = (9.428)(10^{-5})(4/\pi N_c)/\ (K_6 C_s). \qquad (48)$$

Consider the implicit function $h_1(c_r^+, v^-, b, d_I^+, d_E^+, r) = 0$ defined by the equality constraint. If we use it to solve implicitly for d_E we get $d_E = \phi_1(c_r^-, v^+, b, d_I^-, r)$ based on the implicit function theorem (Papalambros and Wilde 1988). Eliminating d_E implicitly from Model B1 we get the same model functions except that h_1 is not present and g_3, g_4, g_5 are replaced by

$$g_3'(b, d_I, c_r^+, v^-, r) \leq 0$$
$$g_4'(d_I^+, c_r^+, v^-, b, r) \leq 0$$
$$g_5'(d_I^-, c_r^-, v^+, b, r) \leq 0 \qquad (49)$$

By MP1 wrt d_I at least one of g_3' or g_4' must be active, while by MP2 wrt r at least two of the above three constraints must be active. Since g_4' and g_5' cannot be simultaneously active g_3 is definitely active, but it cannot be concluded at this point that both g_3 and g_4 must be active as in the case for flat heads. However, the problem has now one less variable and one less constraint. This completes the model analysis and the analytical results will be highlighted in the context of the numerical results.

3.3 The Optimizer NLPQL (NCONF).

The NLPQL algorithm (Schittkowski, 1986) is available as a subroutine in the International Mathematical and Statistical Library (IMSL) [IMSL 1991] under the names NCONF and NCONG. It has been designed to solve the general nonlinear programming problem :

$$\begin{aligned} &\min f(\mathbf{x}) \\ &\text{subject to: } g_j(\mathbf{x}) = 0 \qquad j=1,\dots,m_e \\ &\qquad g_j(\mathbf{x}) \geq 0 \qquad j=m_e+1, \dots, m \qquad (50) \\ &\qquad \mathbf{x_l} \leq \mathbf{x} \leq \mathbf{x_u} \end{aligned}$$

Note the change in notation from Section 2 for the name of the equality constraint set and for the sign on the inequality constraint set. Also, note that variable bounds are specified separately from the constraint set. These changes are noted only to be consistent with the reference manuals on the algorithm.

It is assumed that all problem functions are continuously differentiable. The NLPQL algorithm realizes a sequential quadratic programming method, also called recursive quadratic programming, constrained variable metric, or the algorithm of Powell [1978]. In each iteration a quadratic programming subproblem is formulated by linearizing the constraints and approximating the corresponding Lagrange function quadratically. A new iterate is calculated then by minimizing a so-called merit or penalty function along the search direction obtained from the subproblem. The Hessian matrix of the Lagrange function is approximated by the Broyden-Fletcher-Goldfarb-Shanno (BFGS) method. (See Papalambros and Wilde, [1988] p. 340 for a description of the BFGS method.)

The main program that calls NCONF must contain an array of design variables, upper and lower bounds on those variables, and subroutines NLFUNC and NLGRAD. NLFUNC calculates and returns the values of objective function and constraints at given variable values. NLGRAD calculates the gradient of the objective function and constraints with respect to the design variables using a forward difference approximation of the partial derivative. NLGRAD calls NLFUNC for the forward difference calculation. Subroutines that calculate the gradient using other methods (including the analytical derivative if available) can be used in place of NLGRAD.

3.4 Engine System Assessment Model

The Engine System Assessment (ESA) program contains more comprehensive expressions than the analytical models given above. For example, it implements the friction model given by Patton et al. [1989]. Input engine geometry is described by 72 quantities, ten of which have continuous values; the remaining values are discrete and reflect specific design configurations. Examples of discrete-valued quantities are the number of cylinders, number of piston rings, and multipliers that reflect specific component types such as a roller finger follower valvetrain. Outputs include a measure of WOT performance (volumetric efficiency or torque) as a function of engine speed, analogous to the base volumetric efficiency curve in the analytical model, as well as the other engine performance quantities used in the analytical models above.

3.5 The ESA-NLPQL Interface

Coupling ESA and NCONF requires a means to pass variable values to ESA, call ESA from NCONF, and access ESA output. Three keys to the coupling are the ability to run ESA with a batch file, a 400 element array in ESA that contains all input and output data, and the use of a single file called the problem definition file ('prob.def'). Appendix A shows the file contents with descriptions. Figure 3 shows a schematic of the interface and data flow through the various subroutines. The main program performs three functions: it reads the problem definition file using a subroutine called LOADPROB; it initializes the variables and sets bounds based on the contents of 'prob.def'; and it invokes the optimizer subroutine NCONF once. NCONF invokes calls to NLFUNC to perform function evaluations and gradient evaluations. NCONF is the only subroutine that invokes ESA. This is accomplished by calling WRITE_INPUT to build a batch file to run ESA with the appropriate variable values; invoking a shell script to run ESA; and then reading the contents of the 400 element array stored in 'dump.tmp'. The objective function and constraints are evaluated with the relevant contents of the array.

The design optimization model that uses ESA as the underlying analysis model is identical to Model A with several exceptions. ESA serves now as an implicit function generator for the NLPQL optimizer. ESA is capable of providing peak power and RPM of peak power as output. This feature is exploited to minimize computational time during optimization iterations. The variable w (RPM) still appears in constraint g_8 but only as an implicit function of the other four design variables.

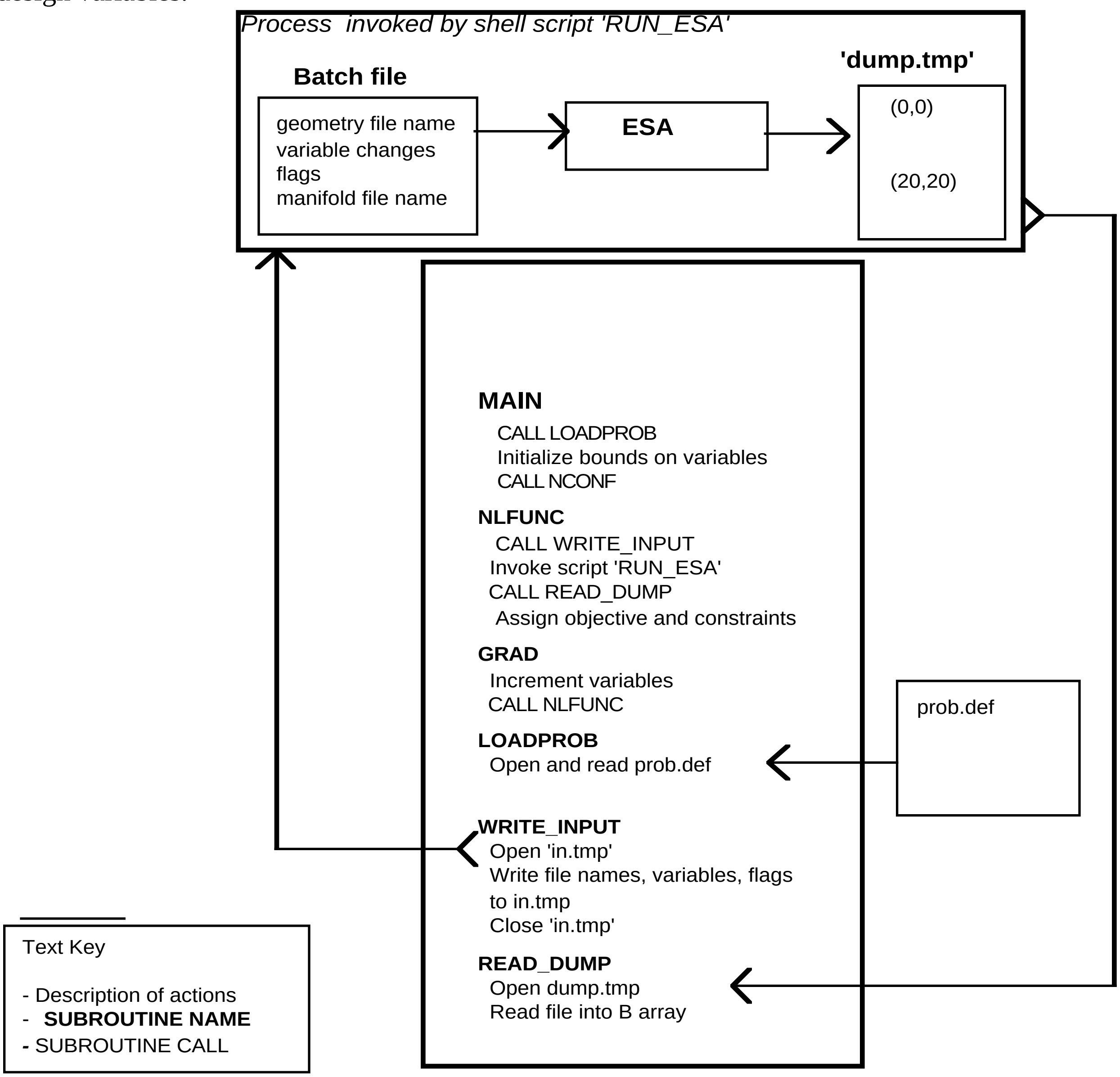

Figure 3. Schematic of ESA/NCONF interface.

The problem statement presented to the optimizer is as follows:

MODEL C (51)

Minimize $BKW/V = f_{1esa}(b, d_I, d_E, c_r; A_f = 13.5, MAP = 99.63 \text{ kPa})$ (in kW/liter)

subject to

$g_1 = K_1 N_c b - L_1 \leq 0$ — min bore wall thickness

$g_2 = (4K_2 V/\pi N_c L_2)^{1/2} - b \leq 0$ — max engine height

$g_3 = d_I + d_E - K_3 b \leq 0$ — valve geometry and structure

$g_4 = K_4 d_I - d_E \leq 0$ — min valve diameter ratio

$g_5 = d_E - K_5 d_I \leq 0$ — max valve diameter ratio

$g_6 = (9.428)(10^{-5})(4V/\pi N_c)(w/d_I^2) - K_6 C_s \leq 0$ — max port/chamber Mach Index

$g_7 = c_r - 13.2 + 0.045\, b \leq 0$ — knock-limited compression ratio

$g_8 = w_{esa}(f_{1esa}) - K_7 \leq 0$ — max torque converter rpm

$g_9 = (isfc)_{esa} - K8 \leq 0$ — min fuel economy at part load

where

$(isfc)_{esa} = f_{2esa}(c_r, b; A_f = 14.6, BMEP = 262 \text{ kPa}, RPM = 1500, EGR = 0\%)$

The implicit function f_{1esa} is a subroutine call that builds the ESA input files, invokes the ESA program at WOT conditions, and extracts the peak power density and the w at peak power from the available output. The implicit function f_{2esa} is a subroutine call similar to f_{1esa} that runs tthe ESA program at the part throttle condition and extracts the specific fuel consumption from the outputs. The variables in this functions and parameter value settings used are indicated in the model above. Note that ESA is called twice for each function call made by NLPQL.

4. Computational Results and Parametric Studies

Subroutine NLPQL was used to solve Models A1, B1, and C numerically. Post-optimal parametric studies were performed to examine the sensitivity of the optimal solution with respect to some key parameter values. Only some parametric results are presented below. Many different combinations of parameters can be examined, as long as the model validity assumptions are not violated.

Note that as NLPQL is capable of identifying only local solutions that satisfy the Karush-Kuhn-Tucker (KKT) first-order optimality conditions, it is possible that the solutions indicated are saddlepoints rather than minima. However, the preceding model analysis that led to constraint activity identification is a strong safeguard against this possibility.

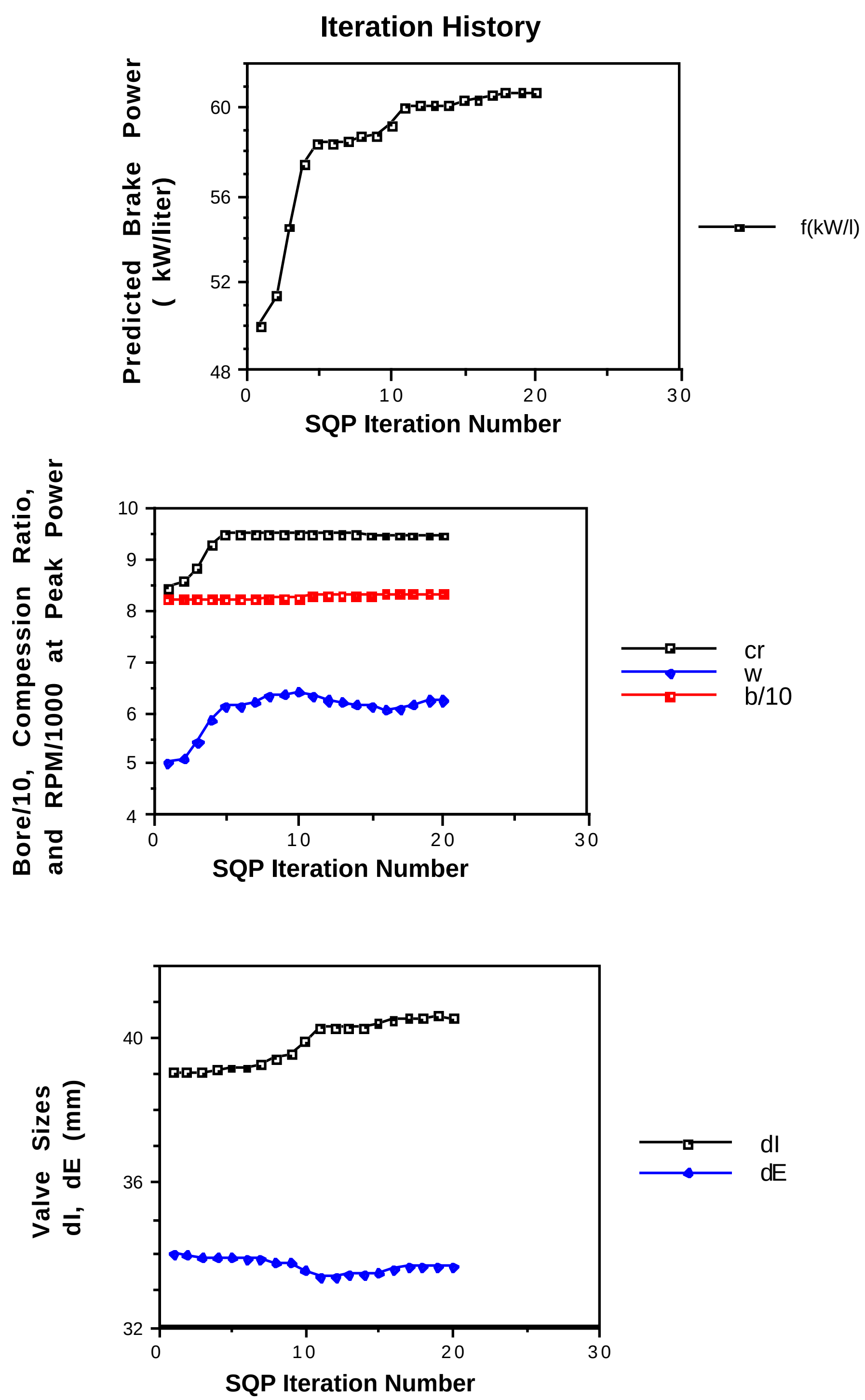

Figure 4. Search History of Optimization Algorithm Using Algebraic Model of Flat Head Chamber (Model A1).

4.1 Optimal Designs: Models A1, B1, and C

Results for the "base case" of parameter values indicated in Tables 3 and 4 are presented first. For flat head geometry Table 6 shows initial and final (optimal) values obtained by NLPQL after twenty iterations. The iteration history is shown in Figure 4, as a typical example of the search pursued by the optimizer. Note that an SQP method will obtain intermediate infeasible results as part of its strategy.

Table 6. Flat Head Geometry Results

	Power Density f (kW/l)	Bore b (mm)	Intake Valve Diameter d_I (mm)	Exhaust Valve Diameter d_E (mm)	Compression Ratio c_r	RPM w*1000
Starting Point	50.02	82.0	39.0	34.0	8.42	5000
Final Point	60.7	83.3	40.5	33.6	9.45	6230

Some observations on these results are as follows. At the initial design the value of RPM is not that of peak power and the value of cr is not the knock-limited compression ratio. The active constraints for the final design are the upper bound on bore wall thickness g_1, the geometric relationship between valves and bore g_3, the minimum valve diameter ratio g_4, and the knock-limited compression ratio g_7. Activities for g_3 and g_4 were proven by monotonicity analysis. For the initial geometry, w = 6.13 (6130 rpm) and f = 55.52 kW/l at the peak power point. The optimal design increases peak power to 60.7 kW/l at 6230 rpm; a 9.3 % improvement. The activity of the knock-limited compression ratio accounts for about half of the increase. The remainder of the increase is attributable to increased flow area (larger bore) and increased engine speed (shorter stroke).

Results for the compound valve geometry are shown in Table 7 and Table 8. For the results in Table 7, the displacement is a parameter (fixed) and the objective is again maximum power density. The constraints on minimum bore wall thickness (g1), maximum engine height (g2) , and the knock limited compression ratio (g7) are active. The compound valve head results in a larger valve size, which results in higher predicted peak power.

Typically, power density is chosen as an objective because of the assumption that displacement volume scales with package constraint. However, if the package constraints can be specified explicitly for the engine problem, this assumption is not required and displacement volume can be treated as a variable. Then, net power, not net power density is a more appropriate objective function. Model B was rerun with displacement volume as a variable to illustrate this effect. The result is shown in Table 8. The optimal power density is reduced to 61.5 kW/l; the net power for the *package* improved by 10% over the optimal design in Table 7. Clearly, power per *package* displacement is a more appropriate objective function than power per *engine* displacement.

Table 7. Compound Valve Head Results (constant volume)

	Power Density f (kW/l)	Bore b (mm)	Inlet Valve Diameter d_I (mm)	Exhaust Valve Diameter d_E (mm)	Head Radius r (mm)	RPM w*1000	Displacement Volume (constant) v (l)
Starting Point	54.94	82.0	39.0	34.0	50.0	5000	1.859
Final Point	65.6	83.3	46.44	37.0	56.5	6240	1.859

Table 8. Compound Valve Geometry Results (Variable Volume)

	Power f (kW)	Bore b (mm)	Inlet Valve Diameter d_I (mm)	Exhaust Valve Diameter d_E (mm)	Head Radius r(mm)	RPM w*1000	Displacement Volume v (l)
Starting Point	117	82.0	39.0	34.0	50.0	5000	1.859
Final Point	134	83.3	46.44	38.5	50.8	6240	2.180

The initial results obtained with the implicit ESA model are shown in Table 9. NLPQL found a convergent solution to this problem in three iterations. The active constraints are the bore wall thickness g_1, the geometric relationship between valves and bore g_3, the minimum valve diameter ratio g_4, and the knock-limited compression ratio g_7. For the starting design, w = 4.8 (4800 rpm) and f = 38.4 kW/l at the peak power point. The constraint activity was identical to the results for MODEL A1. The differences in the solutions are the optimal values of f and w. The absence of significant elements of the friction expression in Model A1 accounts for the difference in objective function. The difference in base volumetric efficiency curves between Model A1 and Model C accounts for the differences in w. Model C used an experimentally measured volumetric efficiency with w = 4.0 (4000 rpm); the base volumetric efficiency curve for Model A1 peaks at w = 5.25 (5250) rpm. The optimal design obtained using Model C increases peak power relative to the baseline by 11.5 %. Again, the activity of the knock-limited compression ratio accounts for about half of the increase and the remainder is attributable to increased flow area (larger bore) and increased engine speed (shorter stroke).

Table 9. ESA -based Results

	Power Density f (kW/l)	Bore b (mm)	Inlet Valve Diameter d_I (mm)	Exhaust Valve Diameter d_E (mm)	Compression Ratio c_r	RPM w*1000
Starting Point	36.67	82.0	39.0	34.0	8.42	5000
Final Point	40.9	83.3	40.5	33.6	9.45	5200

4.2 Sensitivity of Optimal Designs to Constraint Parameters

We now examine the effect of changing parameter values on the optimal solutions. For flat head chamber design (Model A1), parameter P_1 appearing in constraint g_1 contains the effect of limiting engine length and the structural design rule for minimum cylinder wall thickness. A family of optimal designs, generated by varying P_1 between 83.33 mm and 100.0 mm, is shown in Figure 5. These values can be attained by changing L_1, K_1, or both. The fuel constraint g_9 becomes active when P_1 = 92.67 mm; however, this corresponds to a bore-to-stroke ratio greater than 1.3 which is considered outside the validity domain of the model. Within the valid domain, the dependence of f* with respect to P_1 is nearly linear, and the sensitivity, df*/dP_1 = 0.72 kW/l per mm. Physically this means a 1% relaxation of the package length or a 1% relaxation of the minimum bore wall thickness results in a potential 1% increase in peak power. Therefore this constraint should be chosen judiciously.

The variation of the solution with respect to the constraint on isfc at the world-wide mapping point (K_8) was also examined. The value of P_1 = 83.33 mm imposes a very small feasible domain, so P_1 was relaxed to 90.91 mm (K_1 was set to 1.1) and K_8 was varied between 219 and 242 g/kWh (i.e., $\pm$ 5% of the base value). The sensitivity of the optimal design to this upper bound is shown in Figure 6. For K_8 > 228.8 g/kW-hr, the constraint g_9 is satisfied as an inequality (it is inactive) and the solution does not change with K8. For K_8 between 219 and 228.8 g/kW-hr, the solution changes. The dependence of the design on K8 is represented as a second order polynomial fit of f*(K_8). To first order, the sensitivity of f* wrt K_8 is 1.35 kW/l per g/kWh. This roughly translates to 4% decrease in peak power per 1% decrease in specific fuel consumption.

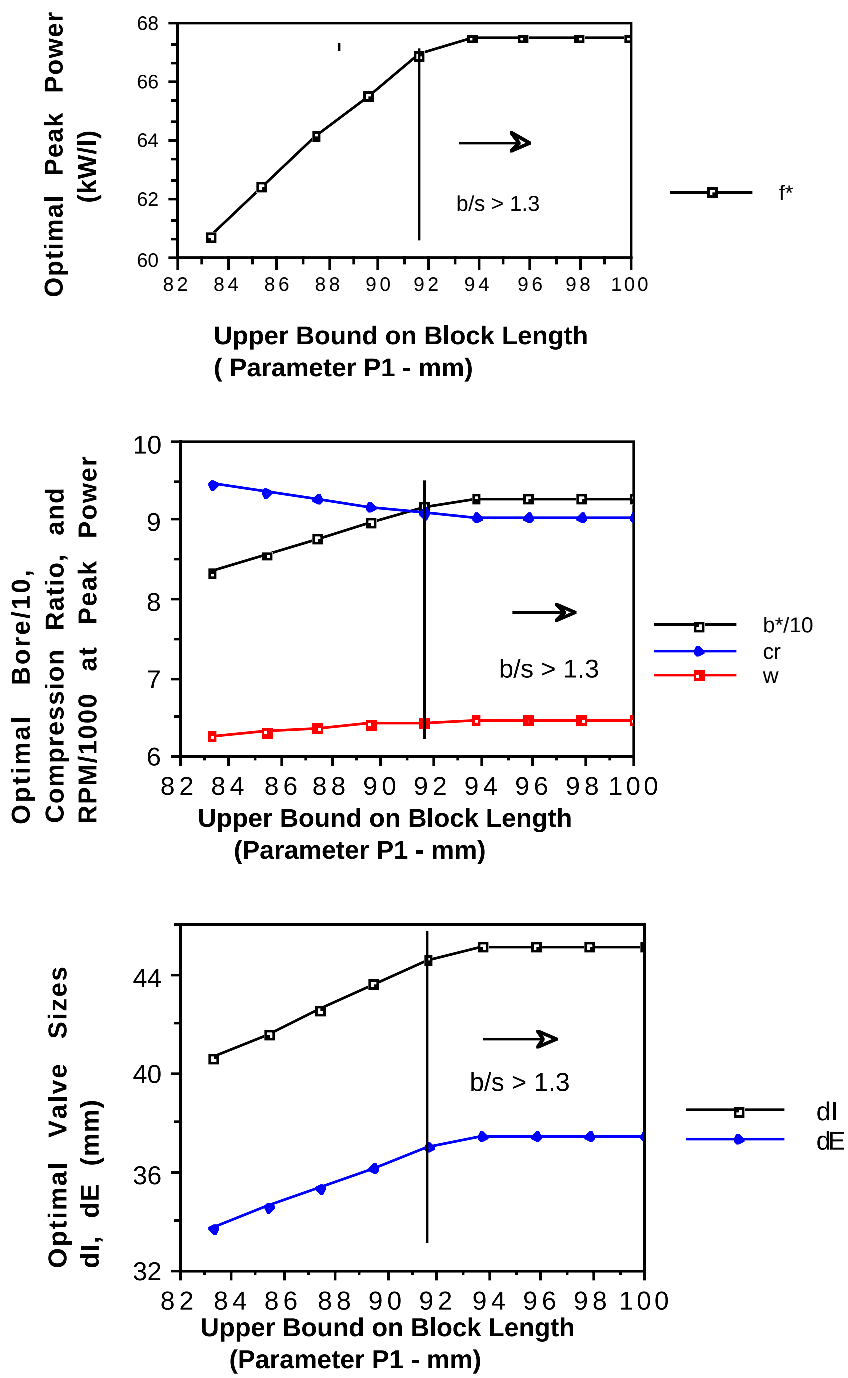

Figure 5. Optimal Design for Algebraic Flat Head Model (A1) as a Function of Upper Bound on Package Length - P_1 (mm) (K3 = 0.82; K8 = 230.5 g/kW-hr).

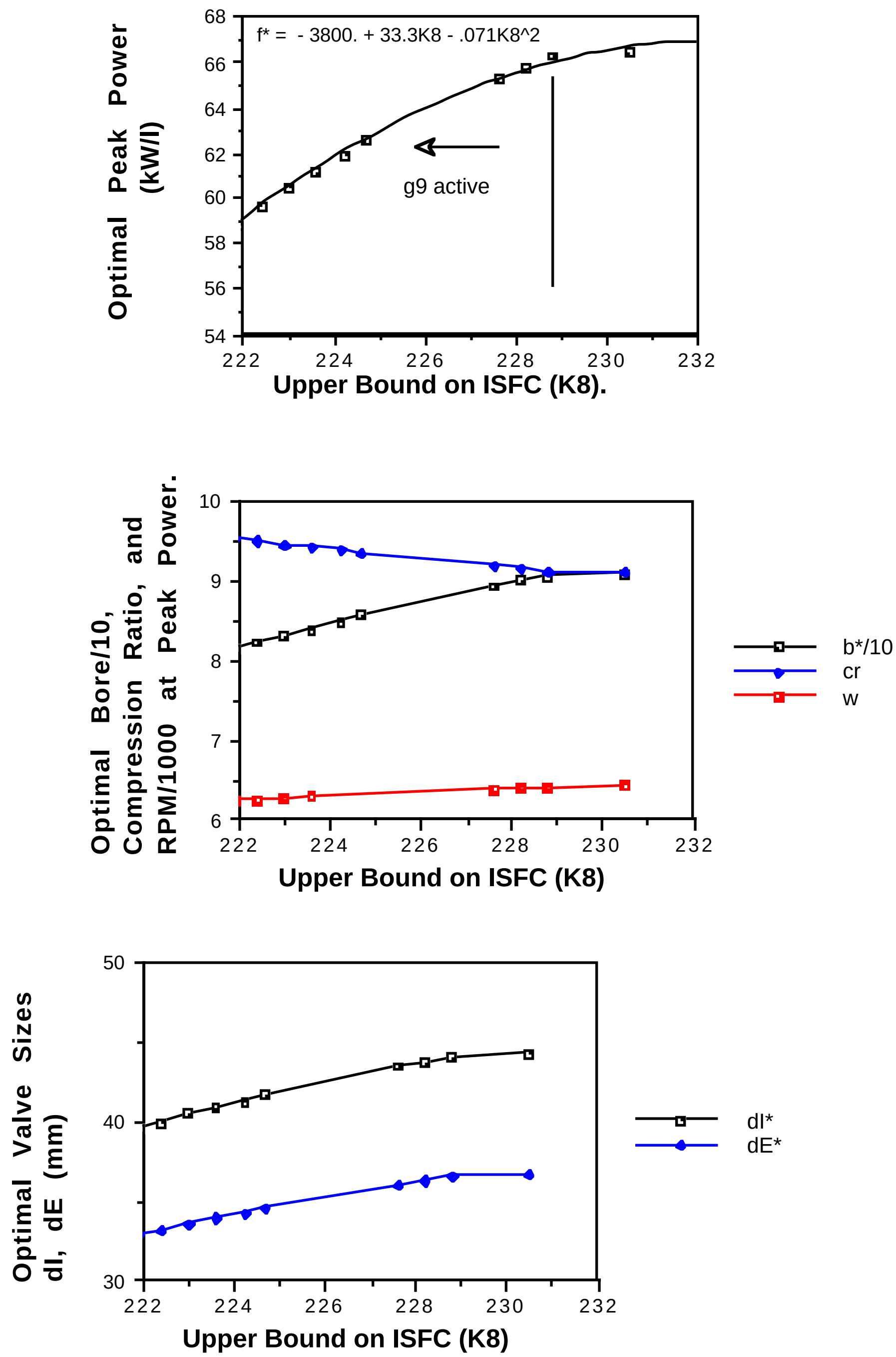

Figure 6. Optimal Design for Algebraic Flat Head Model (A1) as a Function of Upper Bound on ISFC - K8 (g/kW-hr). (K3 = .82; P1 = 90.91 mm).

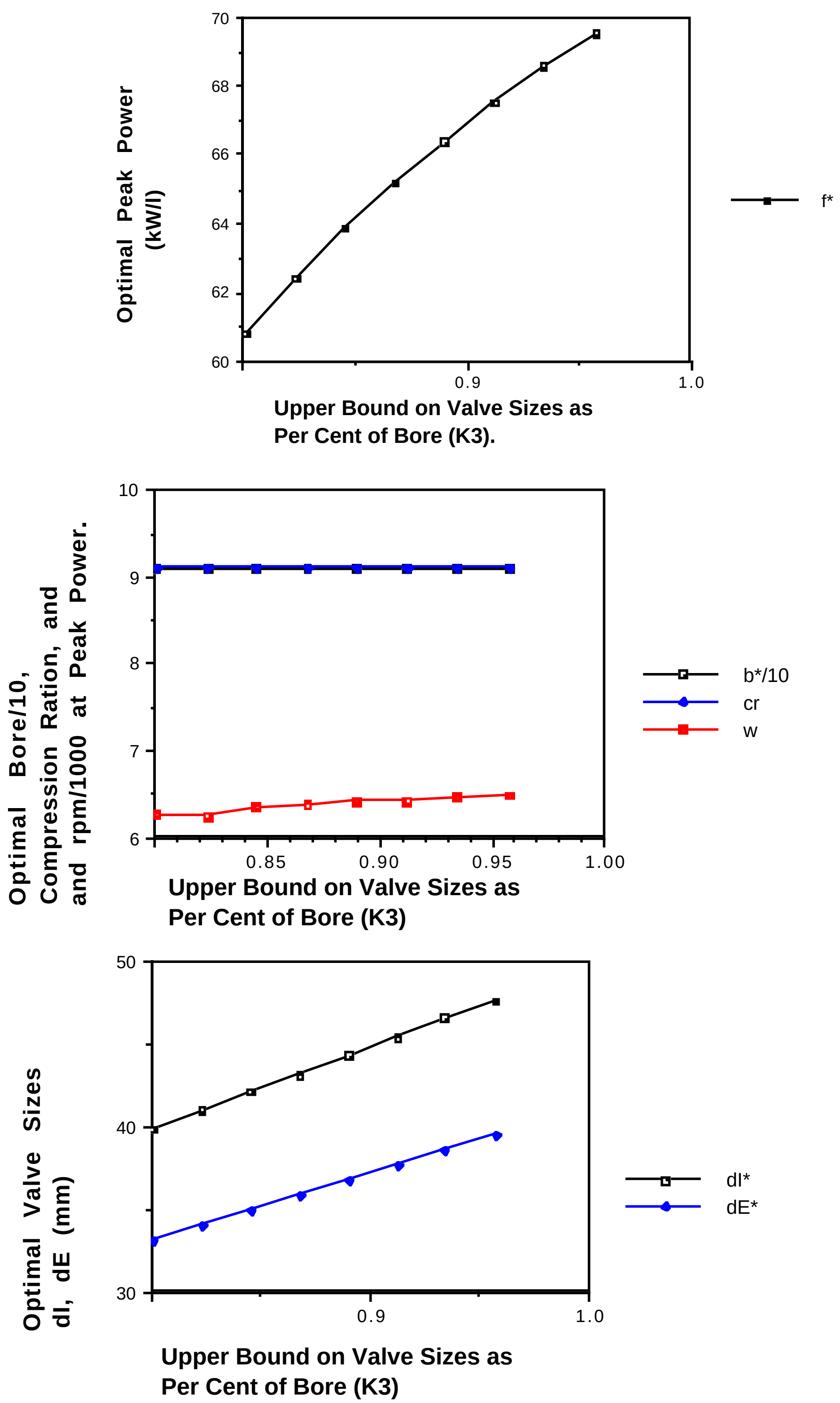

Figure 7. Optimal Design for Algebraic Flat Head Model (A1) as a Function of Upper Bound on Total Valve /Bore Ratio (K8 = 230.5 g/kW-hr; P1 = 90.91 mm).

Parameter K_3, which reflects the geometric relationship between the valves and the bore, was also varied to generate a family of optimal designs as shown in Figure 7. No change in constraint activity was observed over the parameter range. The relationship between f* and K_3 is nearly linear. This constraint should also be chosen very judiciously, because the sensitivity df*/dK3 = 6 kW/l implies that a 1% change in K_3 is roughly equivalent to a 1% change in optimal net power.

Identical parametric studies were conducted using Model C. These results are summarized in Figures 8, 9, and 10. Figure 8 shows the variation of the optimal design with the package length P_1(mm). The fuel constraint becomes active at P_1 = 93.78 mm (not shown) which is beyond the validity of the model (b/s > 1.3). The sensitivity df*/dP1 = 0.4 kW/l per mm implies that a 2% increase in package length can yield a 1% increase in peak power.

The lower sensitivity (relative to Model A1) is due to the lower absolute values of f*, a direct result of the more complete friction model in Model C (the ESA program). Figure 9 shows the variation of optimal designs predicted by Model C with respect to the upper bound on the isfc constraint, K8 (with P1 = 90.91). The fuel consumption constraint, g_9 becomes active at K8 = 228 g/kW-hr. The sensitivity of f* with respect to K8 says that roughly to a 1% improvement in specific fuel (1% decrease in K8) results in a 4.5% decrease in peak power.

Figure 10 shows the variation of optimal peak power with the ratio of valve size to bore, K3. The parameter K3 had no effect on constraint activity over the range investigated; hence, only the optimal values of valve sizes varied linearly with K3. A 1% increase in the ratio K3 results in a 1% increase peak power in the optimal design.

The utility of the approach presented is not that it provides a *single* solution but, that, once the optimal design problem is cast, it yields a family of design solutions with quantitative assessments of design compromise. For example, the results in Figure 8 show that allowing an increase in block length of 4 mm may result in a potential gain of 0.5% power. Such information is essential for good synthesized design. Similarly, Figure 9 illustrates that a 1% improvement in part load fuel consumption requires giving up 4% in power. The trade-off between fuel consumption and power is qualitatively intuitive; this approach also yields a quantitative assessment.

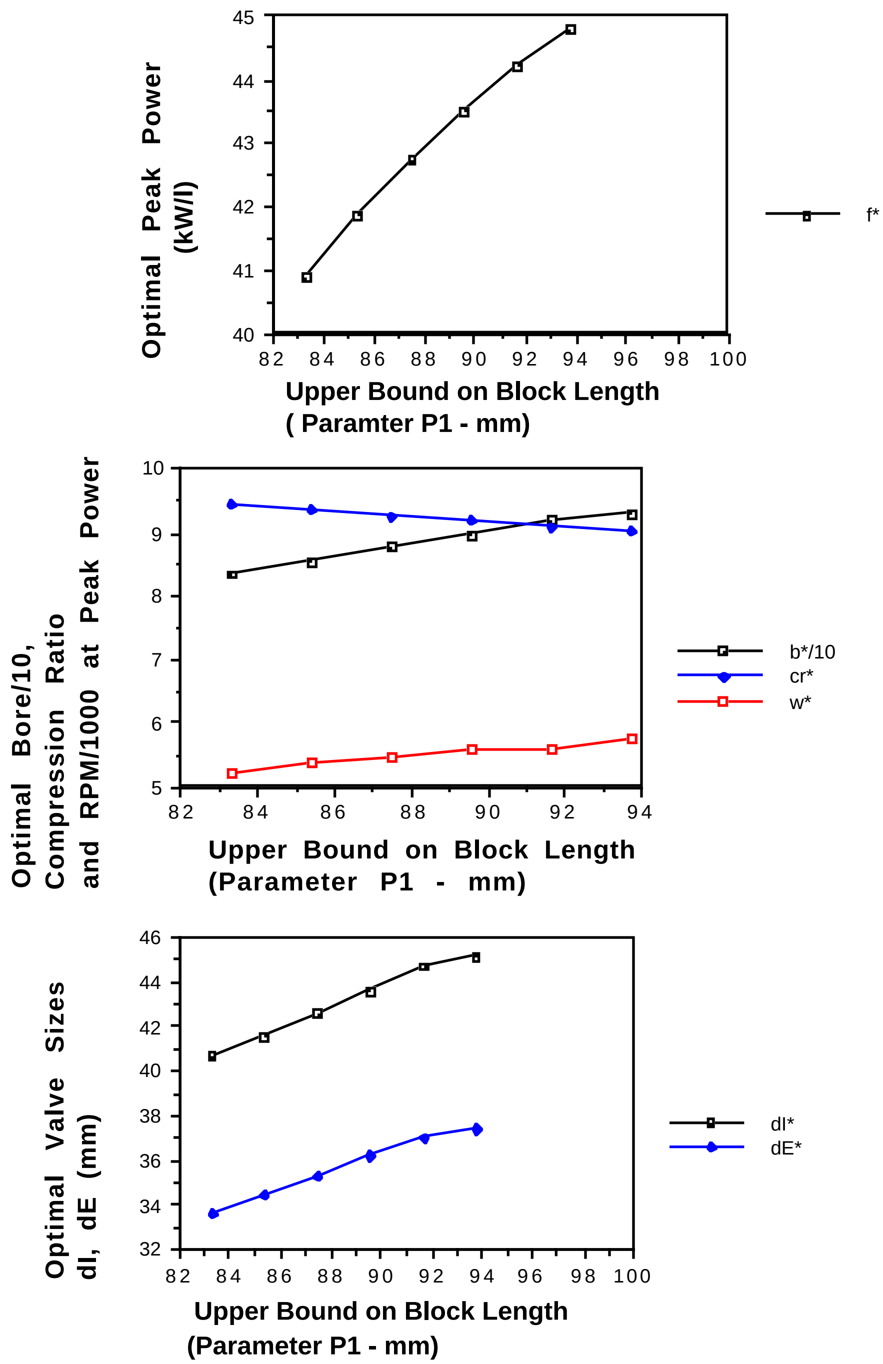

Figure 8. Variation of ESA Based Optimal Design (Model C) as a Function of Upper Bound on Package Length - P1 (mm) (K3 = 0.82 ; K8 = 230.5 g/kW-hr).

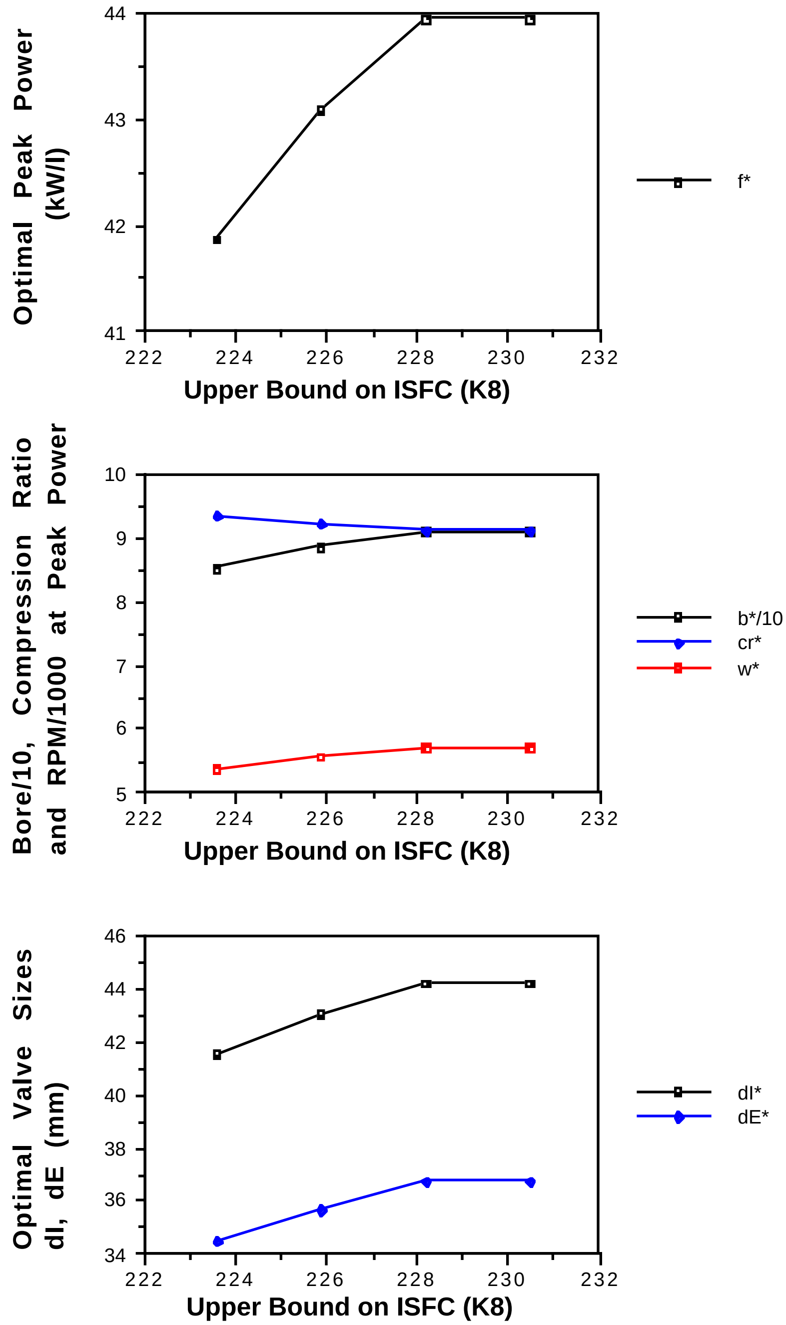

Figure 9. Variation of ESA Based Optimal Design (Model C) as a Function of Upper Bound on ISFC - K8 (g/kW-hr) (K3 = 0.82; P1 = 90.91 mm).

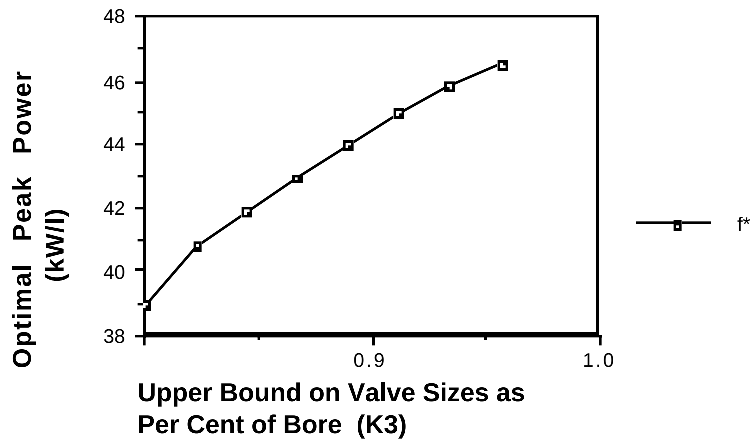

Figure 10. Variation of ESA Based Optimal Design (Model C) as a Function of Upper Bound on Total Valve/Bore Ratio - K3 (K8 = 230.5 g/kW-hr); P1 = 90.91 mm).

CONCLUSIONS

Monotonicity analysis and a sequential quadratic programming algorithm produced predictions of the optimal combustion chamber geometry using three engine models of increasing complexity. The models produced similar trends but different values of objective function, which affected constraint activity. The predictions indicate that a maximum bore/stroke ratio is required for maximum power/liter for a fixed displacement engine. In this problem formulation, the maximum bore was determined by the activity of either the package constraint or the fuel consumption constraint.

The increased bore size results in increased flow area per unit displacement and reduced stroke. This in turn has the effect of shifting the peak of the power curve to higher speeds at comparable torques and it results in higher peak power. Realizing the benefits of this increased power in a vehicle may require redesign of a transmission. In fact, current design practice tends to place substantially tighter bounds on the speed of peak power simply because of transmission design change costs.

Clearly, numerous design scenarios can be studied. Fuel consumption could be treated as an objective, and power as a constraint. Additional constraints representing emissions could (and should) be formulated to generate more representative design rules. This paper has demonstrated the advantages of coupling a numerical optimization scheme to an existing engine model program.

The utility of such an approach with more complex models like ENGSIM is apparent. Since NLQPL and similar algorithms require the objective function and constraints to be differentiable, an algebraic representation of ENGSIM output is desirable. A possible approach is to use the algebraic equations generated by Kenney's method [1989] to solve a reasonably difficult design problem. Currently, a ten variable problem that relies on ENGSIM output is considered difficult. This approach will be explored and should be useful for studying solutions to current engine design problems.

ACKNOWLEDGEMENTS

The authors are grateful to Mr. Rich Belaire and Mr. Brad Boyer for their invaluable assistance with implementing the ESA program. This research has been partially supported by a Ford Motor Co. grant to the University of Michigan. This support is gratefully acknowledged.

REFERENCES

Auiler, J.E., Zbrozek, J.D., Blumberg, P.N., 1977, "Optimization of Automotive Engine Calibration for Better Fuel Economy - Methods and Applications", SAE Paper No. 770076, SAE International Congress, Detroit, MI.

Assanis, D.N., and Polishak, M. 1989, "Valve Event Optimization in a Spark Ignition Engine", ASME Transactions, Internal Combustion Engines, Vol. 9, pp.201-208.

Belaire, R.C., and Tabaczynski, R.J., 1985, "The Engine System Assessment User's Guide", Ford Research Report No. SR85-141.

Bishop, I.N., 1964, "Effect of Design Variables on Friction and Economy", SAE Paper 812a presented at the SAE Automotive Engineering Congress, January, Detroit, MI.

Blumberg, P.N., Lavoie, G.A., and Tabaczynski, R.J., 1980, "Phenomenological Models for Reciprocating Internal Combustion Engines", *Progress in Energy and Combustion Science* , Vol. 5 .

Borgnakke, C., Davis, G.C., and Tabaczynski, R.J., 1981, "Predictions of In-Cylinder Velocity and Turbulence Intensity for an Open Chamber Cup-in-Piston Engine", SAE Transactions, Paper No. 810224, 1981.

Campbell, A.S., 1979, *Thermodynamic Analysis of Combustion Engines*, Krieger, Malabar, Florida.

Chapman, M., Novak, J. M., and Stein, R. A., 1982,"Numerical Modelling of Inlet and Exhaust Flows in Multi-cylinder Internal Combustion Engines", ASME Fluids Engineering Division Meeting, Phoenix, AZ, November 14-19.

Davis, G.C., and Borgnakke, C., 1982. "The Effect of In-Cylinder Flow Processes (swirl, squish, and turbulence intensity) on Engine Efficiency - Model Predictions", SAE Transactions, Paper No. 820045.

Davis, G.C., Mikulec, A., Kent, J.C., and Tabaczynski, R.J., 1986,"Modeling the Effect of Swirl on Turbulence Intensity and Burn Rate in S. I. Engines and Comparison with Experiment", SAE Paper No. 860325, SAE International Congress, Detroit, MI.

Davis, G.C., and Tabaczynski, R.J., 1988,"The Effect of Inlet Velocity Distribution and Magnitude on In-Cylinder Turbulence Intensity and Burn Rate - Model vs. Experiment", *Journal of Engineering for Gas Turbines and Power*, Vol. 110, pp. 509-514.

Dennis, J. E., and Schnabel, R.B., 1989, "Numerical Methods for Unconstrained Optimization and Nonlinear Equations", Prentice-Hall, Englewood-Cliffs, NJ.

Heywood, J.B., 1980,"Engine Combustion Modelling - An Overview", *Combustion Modeling in Reciprocating Engines*, ed. J.N. Mattavi, C.A. Amann, Plenum Press.

Heywood, J.B., 1988, *Internal Combustion Engine Fundamentals,* McGraw-Hill, New York, NY.

International Mathematical Subroutine Library (IMSL) Math/Library User's Manual - Version 1.1, 1989 , pp 895-900.

Kenney, T. , Latty, C., Maurin, P. , A. Musienko, "Experimental Design for Camshaft Optimization", Presented at Quality Technology Symposium, Ford Motor Company, 24 May, 1989.

Kreiger, R.B., 1980, "Applications of Combustion Models", Combustion Modeling in Reciprocating Engines, ed. J.N. Mattavi, C.A. Amann, Plenum Press.

Luenberger, D.G., 1984, *Introduction to Linear and Non-linear Programming*, Addison-Wesley, Reading Massachusetts.

Newman, C. E., Stein, R. A., Warren, C. C. and Davis, G. C., 1989, "The Effects of Load Control with Port Throttling at Idle - Measurements and Analyses", SAE Paper No. 890679.

Patton, K.J., Nitschke, R.G., and Heywood, J.B., 1989, "Development and Evaluation of a Friction Model for Spark Ignition Engines", SAE Paper No. 890386, SAE International Congress, Detroit, MI.

Papalambros, P. Y. and Wilde, D.J., 1988, *Principles of Optimum Design: Modeling and Computation*, Chapter 4.,

Poulos, S. B., Heywood, J.B.,1983, "The Effect of Chamber Geometry on Spark Ignition Engine Combustion", SAE Paper No. 830334.

Powell, M.J.D., 1978, "A fast algorithm for nonlinearly constrained optimization calculations", *Numerical Analysis*, ed. G.A.Watson, Lecture Notes in Mathematics 630, Springer-Verlag, Berlin.

Press, W.H., Flannery, B.P., Teukolsky, S.A., Vetterling, W.T., 1987, *Numerical Recipes - The Art of Scientific Computing*, Cambridge Press, New York, NY.

Reynolds, W.C., 1980, "Modelling of Fluid Motions in Engines - An Introductory Overview", *Combustion Modeling in Reciprocating Engines*, ed. J.N. Mattavi, C.A. Amann, Plenum Press.

Rishavy, E.A., Hamilton, S.C., Ayers, J.A., and Keane, M.A., 1977, "Engine Control Optimization for Best Fuel Economy with Emission Constraints", SAE Paper No. 770075, SAE International Congress, Detroit, MI.

Schittkowski, K., 1986, "NLPQL: A FORTRAN Subroutine for Solving Constrained Non-linear Programming Problems", ed. C.L.Monma, *Annals of Operations Research*, Vol. 5, pp. 485-500.

Taylor, C.F., 1985, *The Internal Combustion Engine in Theory and Practice: Vol. 1 & Vol II. Second Ed., Revised*, MIT Press, Cambridge, Massachusetts.

Woodard, J. K., Johnson, G. E., and Lott, R. L., 1988, "Automated Design of a Turbocharged, Fueled, Four-stroke, Engine for Minimum Fuel Consumption", ASME Design Automation Conference, Kissimmee, Florida, Sept 25-28.

APPENDIX A

Table AI - Contents of Problem Definition File 'prob.def'.

'prob.def' contents	Data Structure	Description
3	NV	Number of variables
1	NE	Number of equality constraints
3	NC	NE plus and total number of inequality constrai
bore	XDESC(1)	Character descriptors used to build run file
stroke	XDESC(2)	for changing each variable in ESA.
valdii(1)	XDESC(3)	
82., 100., 70.	XINIT(1), BOULOW(1), BOUUPP(1)	Initial value, upper and lower bound of X_1
88., 100., 70.	XINIT(2), BOULOW(2), BOUUPP(2)	Initial value, upper and lower bound of X_2
39., 50., 30.,	XINIT(3), BOULOW(3), BOUUPP(3)	Initial value, upper and lower bound of X_3
3	NO	Number of model outputs to use.
bhp/l 7 4	XDESC(1)	Output descriptor, indices for output
isfc 20 8	XDESC(2)	in 400 element array.
bsfc 20 18	XDESC(3)	